International Journal of Technical Innovation in Modern Engineering & Science (IJTIMES)
Impact Factor: 5.22 (SJIF-2017), e-ISSN: 2455-2585
Volume 5, Issue 1, January-2019

A NEOTERIC APPROACH FOR SHADOW DETECTION IN HIGH RESOLUTION SATELLITE IMAGES

K. Lakshmi Manasa[1], G. Umamaheswara Reddy[2], T.Venkata Krishnamoorthy[3]

1 *M.Tech Student, Department of Electronics and Communication Engineering, Sri Venkateswara University College of Engineering, Tirupati, Andhra Pradesh, India-517502.*
2 *Professor, Department of Electronics and Communication Engineering, Sri Venkateswara University College of Engineering, Tirupati, Andhra Pradesh, India-517502.*
3 *Research Scholar, Department of Electronics and Communication Engineering, Sri Venkateswara University College of Engineering, Tirupati, Andhra Pradesh, India-517502.*

Abstract- High resolution multispectral satellite images contain more information and extracting the region of interest from these images may cause some problems due to the presence of the object shadow. There is some state of art methods for these shadow detection, but doesn't show accurate results due to miss predictions occurs while detecting the shadow regions. In this paper, an image index based on principal component analysis is developed for shadow detection using more than one band. The shadow detector index is used to distinguish between shadow and non shadow pixels based on spectral difference. Shadow pixels are divided from the index histogram by using an automatic threshold identity method. Experimental results show that the proposed method is superior in terms of subjective and objective analysis.

Keywords: Histogram, Automatic threshold, Image index, Principal component, Shadow pixels.

I. INTRODUCTION

Research on remote sensing images is one of the most important topics in the recent years. Utilization of these images is critical to realize the problems and to seek for solutions for many areas such as urban planning, urban growth monitoring, military surveillances, navigation, crop yield estimation, disaster management and traffic management. One of the crucial areas of the remote sensing is shadow detection and it can help to find solution for many problems such as image classification, change detection, tracking etc. In an aerial image the similarity of the classes and the variety of the class obstructs the image classifications. Shadow modifies the radiometric information of the materials and so the objects under the shadow do not indicate their properties. Therefore, without detection of shadows, accurate detection and identification of objects may not be possible.

Shadows are detected either model based or property based. Previous information, such as geometry of 3D scenes and lighting conditions, is required in model based techniques [1]. Although the method has a strong theoretical value, it is limited because the information required is not always easy to obtain. It is not available at all in other cases. The property based method, on the other hand, uses the shadow pixel properties in images and requires no additional information. It is widely used because it is simple and direct. It takes the full advantage of multi-band image spectral features. The index selected from the color model used and the thresholding methods are the two main factors affecting the shadow extraction from the image histogram. The newly developed indices usually consist of a two-band ratio or a multi-band function.

Researchers used several color models for property based shadow detection methods. Sarabandi *et al*. [2] used the color space (C_1, C_2, and C_3) for shadow detection. The (C_3) component is found to be shadow sensitive, so it is used to distinguish shadow from other dark objects in the image. The main problem with the C_3 component, however, is its instability with certain color values, which leads to the misclassification of non-shadow pixels as shadow [1]. Wang and Wang [5] proposed the ratio of the C_3 to the first principle component. However, high-intensity surface characteristics were easily detected as shadows [6]. Besheer and Abdelhafiz [4] improved the original $C_1C_2C_3$ invariant color model with channel information near-infrared (NIR). They used the modified index (C_3^*) for shadow detection. A bimodal histogram threshold is then used to divide the image into shadow and non- shadow. Another successfully normalized saturation value difference index (NSVDI) proposed by Ma *et al*. [8] developed to detect shadows in high-resolution satellite images on the basis of the special properties of shadows in Hue-Saturation-Value (HSV) color space. The last two approaches are used as references in [3] and [9].

II. REGION GROWING METHOD

Shadow detection has obtained sizable interest within the computer vision field, even though now not an awful lot paintings has been finished towards the utility of those consequences to excessive-decision satellite images currently available. In this existing algorithm the principle method is to locate shadows in images, and analyses their suitability for being applied to color satellite imagery. Based on this, it recommends a process that takes advantage of invariant color space and side records to find shadows for pan sharpening images (image resolution up to 1 meter) successfully and correctly.

In the existing region growing method [1], the input image consists mainly of three components, including C_3, intensity and saturation component, and the C_3 component can be multiplied by 3×3 average kernels to neutralize noise from the image, and hence the scale of the gradient of the image may be figured from using the sobel detector. Small spectrums of pixels that are inclined to be shadows are picked as shadow areas seeds. They are often acquired from the local maximum neighborhood in the C_3 aspect of the $C_1C_2C_3$ color area. Each shadow location is then characterized via Gaussian distribution of the C_3 values of the pixels inside this place.

The mean of the intensity (V) aspect of the window's pixels have to be decrease than a positive threshold (T_V) (speculation of shadow darkness). In the identical way, the mean of the saturation (S) element have to be better than a threshold T_S, to keep away from the instability of C_3 for low-saturation colorations. None of the window's pixels belongs to some other preceding seed-window. The process ends when no one of the neighbor pixels has been brought to the place. Notice that, throughout the developing method of a particular seed, pixels of different seed-windows no longer processed yet may be evaluated as any other image pixel.

Limitations

- Miss predictions occur while detecting the shadow regions.
- Accuracy is low.
- Over segmentation due to the region merging technique.

III. PROPOSED METHOD

The proposed approach is designed to define shadow pixels in satellite images of high resolution. Since the use of a single band image shadow pixels are detected inaccurately, it is more convenient to use all the characteristics of the available multispectral image bands in the shadow detection process [7]. Pixels of shadow and non shadow (roads, grounds, buildings and vegetation) react differently at different wavelengths. Therefore, a spectral analysis is able to define shadow pixels [10] in principal. The proposed approach comprises of two stages where a new image index is indeed accumulated to make the distinction between shadow and non-shadow pixels based on the spectral correlation as the first alignment. In the next step, the appropriate threshold is presented to automatically identify the shadow from the index. The following characteristics have the spectral curves of ground features:

1) While the luminosity generally decreases in shadow pixels, it declines sharply in the red band [12].
2) Shadow pixels are saturated with short blue wavelengths due to the atmospheric dispersing effect of Rayleigh [15]. In the blue band, the intensity values of the shadow and non-shadow areas differ the least [10].
3) In the green band, intensity values (I_G) are greater than those in the blue band (I_B) in non-shadow areas ($I_G > I_B$) [11] for most land cover features. The difference in intensities (Δ) in the green band for the same object in shadow and non-shadow is also greater than in the blue band, i.e. $\Delta I_G > \Delta I_B$ [16]. This results in lower values for the term (G–B) in shadow regions comparable to their non-shadow counterparts.
4) While shadow pixels differ slightly between green and blue bands, vegetation pixels differ widely between the two bands.

The schematic diagram of the advanced shadow detector index method is shown in Fig. 1.

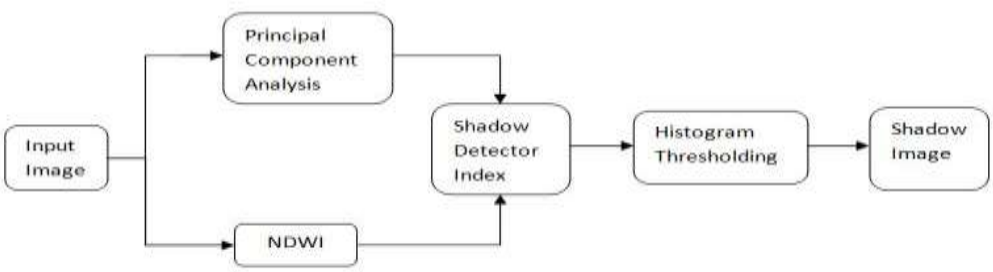

Fig.1 Schematic diagram of advanced shadow detector index method

A. Algorithm for advanced shadow detector index method

1) Consider a pan sharpening satellite image as the input.
2) Calculate the principal components of four bands red, green, blue and NIR (Near-Infrared).
3) Based on the features of the shadow pixels a Shadow Detector Index (SDI) is developed.
4) Calculate Normalized Difference Water Index (NDWI).
5) Add SDI and NDWI to the input satellite image.
6) The histogram is drawn based on the values of the shadow detector index.
7) Apply thresholding technique to divide shadows and non shadows.

In the first step, consider a pan sharpening image and calculate the principal components of four bands red, green, blue and NIR (Near-Infrared) [17]. The first component contains the maximum information represents the major differences in the image between different objects. Based on the features of the shadow pixels a shadow detector index (SDI) is developed. This SDI is applied to the input image. High values are obtained for the shadow regions. The formula is given in the following eq. (1):

$$SDI=\left(\frac{(1-PC_1)+1}{((G-B)*R)+1}\right) \tag{1}$$

Where R, G and B are the normalized values for the red, green and blue bands, respectively. PC_1 is the very first element of the principal component analysis. Maximum information about the spectral bands concentrated on the PC_1 component, i.e. low values for the shadow regions. Dark pixels like vegetation and water pixels are usually misclassified as shadows. The term (G–B) differentiates between shadow pixels (low values) and vegetation pixels (large values) in the SDI index denominator. However on the other hand, water pixels are also categorized as shadows according to the SDI index if they exist. Therefore the water class must be masked in the original image and later applied to the final image of the shadow. The normalized difference water index (NDWI) is explained by Mcfeeter [13] is used for this purpose. The NDWI (Normalized Difference Water Index) is expressed in the following eq. (2):

$$NDWI=\left(\frac{R_G-R_{NIR}}{R_G-R_{NIR}}\right) \tag{2}$$

Where, R_G and R_{NIR} are Green and NIR (Near-Infrared) bands, respectively.

The histogram is drawn based on the values of the shadow detector index. The last right hill in the histogram refers to the shadow pixels and the peak before refers to the non-shadow pixels. Hence by dividing these two peaks at valley point may divide the shadow and non shadow regions. Therefore, need a threshold for this division based on the valley emphasis method [14]. More accuracy was obtained from the method by selecting the threshold value with low probabilities in its neighborhood.

B. Advantages

- Accuracy is high.
- A miss prediction of shadow regions doesn't occur.

IV. RESULTS AND DISCUSSION

In the experiment, firstly used the standard images to analyze the advanced shadow detector index algorithm and the existing region growing algorithm and has been tested to obtain a preliminary comparison. To assess objectively the performance of these two methods, three objective quality measurements, i.e. Accuracy, Mean Square Error (MSE) and Peak Signal to Noise Ratio (PSNR) values for each and every input image are indeed quantified as shown in Table 1, Table 2, and Table 3. In this experiment shows input high resolution satellite images in fig.2 (a), fig.3 (a), fig.4 (a). The existing region growing method results are shown in fig.2 (b), fig.3 (b), fig.4 (b) and the advanced shadow detector index method results are shown in fig.2 (c), fig.3 (c), fig.4 (c).

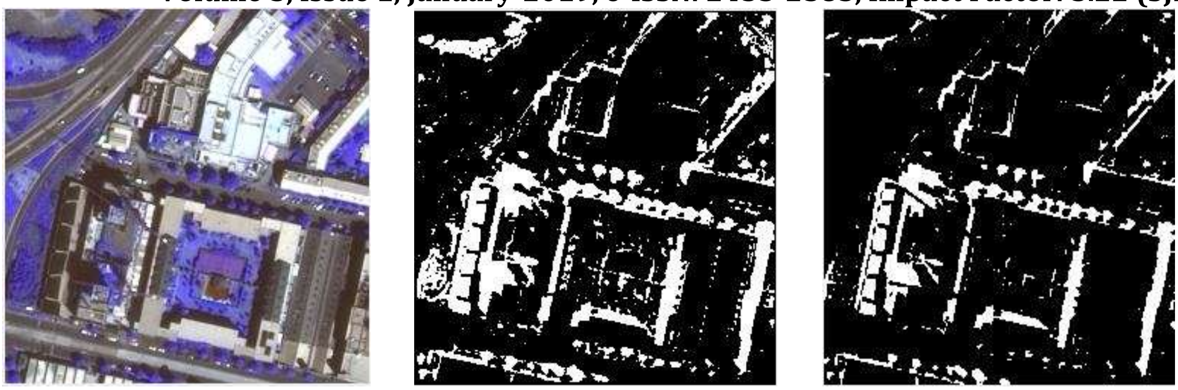

(a) (b) (c)

Fig.2 (a) Input image 1 (b) Shadow detection by Region growing method

(c) Shadow detection by advanced shadow detector index method.

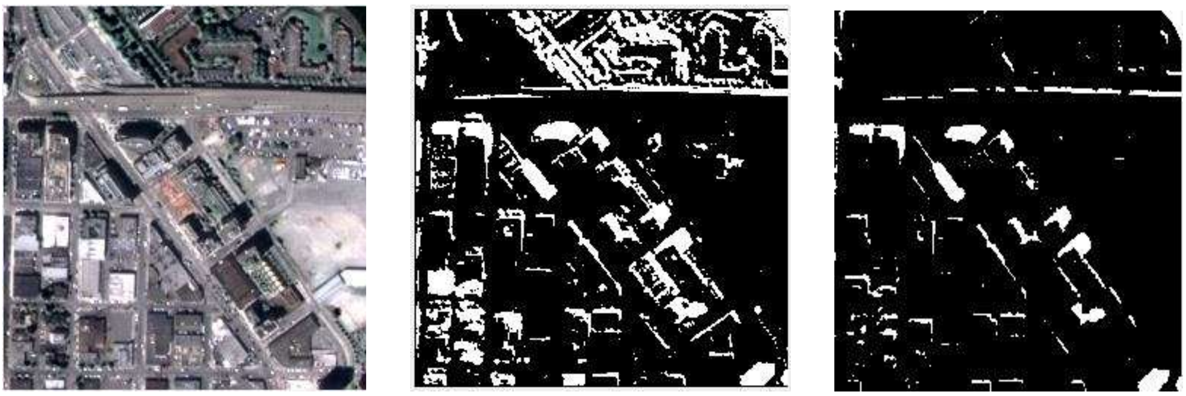

(a) (b) (c)

Fig.3 (a) Input image 2 (b) Shadow detection by region growing method

(c) Shadow detection by advanced shadow detector index method.

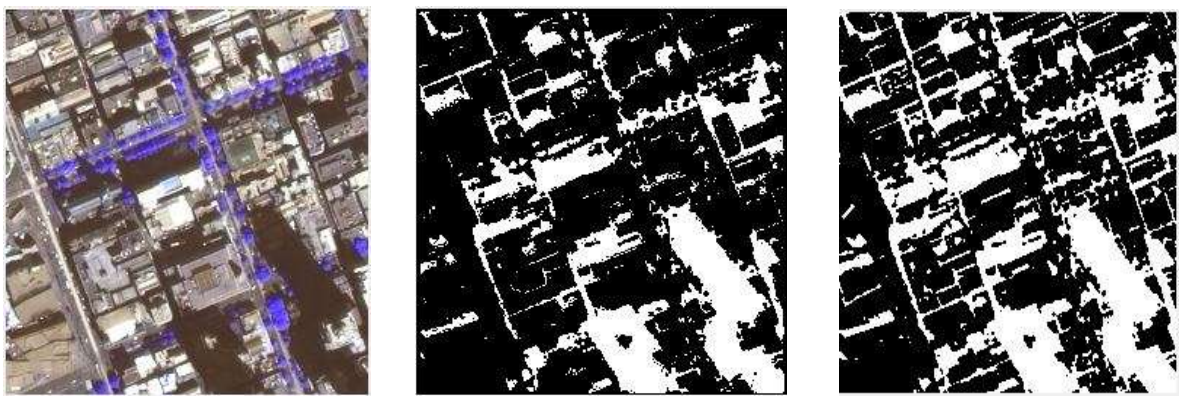

(a) (b) (c)

Fig.4 (a) Input image 3 (b) Shadow detection by region growing method

(c) Shadow detection by advanced shadow detector index method.

A. Quality Metrics

1) *Accuracy:* Accuracy is calculated using below given eq. (3):

$$\text{Accuracy}=\frac{\text{TP+TN}}{\text{TP+TN+FP+FN}} \tag{3}$$

In which, true positive (TP) is number of shadow pixels correctly identified, false negative (FN) is the number of shadow pixels identified as non shadows, false positive (FP) is the number of non shadow pixels identified as shadows, true negative (TN) is the number of non shadow pixels correctly identified, and TP + TN + FP + FN stands for the total number of pixels in the image. The advanced shadow detector index method has more accuracy (average of 85%) than the region growing method as shown in Table.1.

Table 1: Accuracy Values For Existing And Proposed Methods

S.NO	Images	Methods	
		Existing (Region growing)	**Proposed (Advanced SDI)**
1	Image 1	75.96	88.89
2	Image 2	72.36	82.22
3	Image 3	70.53	87.78

2) PSNR (Peak Signal to Noise Ratio):

Usually indexed on a logarithmic (dB) scale, a metric content is often used to quantify the reliability of any restored or corrupted image in relation to its reference or image of ground truth. The Mean Square Error (MSE) and the Peak Signal to Noise Ratio (PSNR) are used to compare the image quality. The lower the values of MSE, the lower the errors. The higher the PSNR, the better the quality of the compressed image.

To compute the PSNR, calculate the mean square error using the below eq. (4):

$$\mathrm{MSE}=\frac{1}{mn}\sum_{i=0}^{m-1}\sum_{j=0}^{n-1}\left[I(i,j)-K(i,j)\right]^2 \tag{4}$$

Where MSE is Mean Square Error, I (i,j) is the input image, K (i,j) is the output image, m and n are the rows and columns of the input image, respectively. Then PSNR is calculated using the following eq. (5):

$$\mathrm{PSNR}=10\times\log_{10}\left(\frac{\mathrm{MAX}_I^2}{\mathrm{MSE}}\right) \tag{5}$$

Where MAX_I is the maximum possible image pixel value. When pixels are expressed using 8 bits per sample, this is 255. More typically, when samples are conveyed using linear PCM with B bits per sample, MAX_I is 2^B-1.

Table 2: Mean Square Error Values Of Existing And Proposed Methods

S.NO	Images	Methods	
		Existing (Region growing)	**Proposed (Advanced SDI)**
1	Image 1	0.5438	0.4020
2	Image 2	0.6769	0.4889
3	Image 3	0.6047	0.2733

Table 3: Peak Signal To Noise Ratio Values Of Existing And Proposed Methods

S.NO	Images	Methods	
		Existing (Region growing) (dB)	Proposed (Advanced SDI) (dB)
1	Image 1	17.720	30.041
2	Image 2	15.972	30.203
3	Image 3	16.963	35.542

For the best results, the mean square error (MSE) should be lower and the PSNR value in dB should be higher. As the data in the Table1, Table 2 and Table 3 shows, the advanced shadow detector index method has a relatively good effect on accuracy, mean square error (MSE), peak signal to noise ratio (PSNR).

V. CONCLUSION

In this paper, a new approach for shadow detection is presented and validated. In the offered approach, an image index, named shadow detector index (SDI), is urbanized. Shadow pixels will achieve high values in the developed index. These pixels are then extracted from the index histogram using a convinced threshold. An average overall accuracy of 85% is obtained by applying the proposed approach on three areas of study with various land cover. The results showed that the rate of truly detected pixels by the advanced shadow detector index approach (average of 85%) is higher than the region growing algorithm (average of 75%) and the other parameters mean square error and peak signal to noise ratio also obtained better results when compared with the region growing method.

ACKNOWLEDGMENT

The Authors are grateful to the Technical Education Quality Improvement Programme, Phase II, Center of Excellence [TEQIP 1.2.1 (CoE)], Sri Venkateswara University College of Engineering, Andhra Pradesh, India for providing software and training equipment.

REFERENCES

[1] V. Arévalo, J. González, and G. Ambrosio, "Shadow detection in colour high-resolution satellite images," *Int. J. Remote Sens.,* 2008, vol. 29, no. 7, pp. 1945–1963.

[2] P. Sarabandi, F. Yamazaki, M. Matsuoka, and A. Kiremidjian, "Shadow detection and radiometric restoration in satellite high resolution images," in *Proc. IEEE IGARSS.*, 2004, vol. 6, pp. 3744–3747.

[3] J. Li, Q. Hu, and M. Ai, "Joint model and observation cues for single image shadow detection," *Int. J. Remote Sens.*, 2016, vol. 8, no. 6, p. 484.

[4] M. Besheer and A. Abdelhafiz, "Modified invariant colour model for shadow detection," *Int. J. Remote Sens.,* 2015, vol. 36, no. 24, pp. 6214–6223.

[5] Y. Wang and S. Wang, "Detection and compensation of shadows in high resolution remote sensing images using PCA," *J. Appl. Sci.*, 2010, vol. 28, no. 2, pp. 136–141.

[6] J. Jianguo, T. Yuan, W. Mifeng, Z. Yingchun, and Y. Ting, "A shadow detection algorithm for remote sensing images," *J. Comput. Inf. Syst.*, 2013, vol. 9, no. 10, pp. 3783–3790.

[7] S. Wang and Y. Wang, "Shadow detection and compensation in high resolution satellite image based on retinex," in *Proc. 5th Int. Conf. Image Graph.*, Xi'an, China, 2009, pp. 209–212.

[8] H. Ma, Q. Qin, and X. Shen, "Shadow segmentation and compensation in high resolution satellite images," in *Proc. IEEE IGARSS*, Jul. 2008, vol. 2, pp. 1036–1039.

[9] H. Song, B. Huang, and K. Zhang, "Shadow detection and reconstruction in high-resolution satellite images via morphological filtering and example-based learning," *IEEE Trans. Geosci. Remote Sens.*, May 2014, vol. 52, no. 5, pp. 2545–2554.

[10] D. Guangyao, G. Huili, Z. Wenji, T. Xinming, and C. Beibei, “An indexbased shadow extraction approach on high-resolution images,” in *Proc. Int. Symp. Satellite Mapping Technol. Appl.*, 2013, pp. 19–26.

[11] M. Herold, D. A. Roberts, M. E. Gardner, and P. E. Dennison, “Spectrometry for urban area remote sensing-Development and analysis of a spectral library from 350 to 2400 nm,” *Remote Sens. Environ.*, 2004, vol. 91, nos. 3–4, pp. 304–319.

[12] Q. Ye, H. Xie, and Q. Xu, “Removing shadows from high-resolution urban aerial images based on color constancy,” in *Proc. Int. Arch. Photogramm., Remote Sens. Spatial Inf. Sci. (ISPRS)*, Melbourne, VIC, Australia, Sep. 2012, vol. 39, pp. 525–530.

[13] S. K. Mcfeeter, “The use of the normalized difference water index (NDWI) in the delineation of open water features,” *Int. J. Remote Sens.*, 1996, vol. 17, no. 7, pp. 1425–1432.

[14] J. L. Fan and B. Lei, “A modified valley-emphasis method for automatic thresholding,” *Pattern Recognit. Lett.*, 2012, vol. 33, no. 6, pp. 703–708.

[15] J. Su, X. Lin, and D. Liu, “An automatic shadow detection and compensation method for remote sensed color images,” in *Proc. 8th Int. Conf. Signal Process.*, Nov. 2006, vol. 2, pp. 1–4.

[16] J. Huang, W. Xie, and L. Tang, “Detection of and compensation for shadows in colored urban aerial images,” in *Proc. 5th World Congr.Intell. Control Autom.*, Jun. 2004, vol. 4, pp. 3098–3100.

[17] T. Venkata Krishnamoorthy and G. Umamaheswara Reddy, “Fusion Enhancement of Multispectral Satellite Image by Using Higher Order Statistics”, *Asian Journal of Scientific Research*, 2018, vol. 11, pp.162-168.

ABOUT THE AUTHORS

K. Lakshmi manasa, M.Tech student in Electronics and Communication Engineering, specialization in Communication Systems, Sri Venkateswara University, Tirupati. She has completed B.Tech in Electronics and Communication Engineering from JNT University, Anantapur. Her areas of interests are image and signal processing.

Dr. G. Umamaheswara Reddy is currently working as a Professor in the Department of Electronics and Communication Engineering at Sri Venkateswara University, Tirupati, Andhra Pradesh, India. He has completed B.Tech in Electronics and Communication Engineering, M.Tech in Instrumentation & Control Systems, and obtained Ph.D. from Sri Venkateswara University, Tirupati, India. He is a member of ISTE, IE, and BMSI. He has a teaching experience of more than 20 years and has 16 technical publications in National & International Journals. His areas of interest include Signal Processing and Biomedical Signal Processing.

T. Venkata Krishnamoorthy is a Research Scholar in the Department of Electronics and Communication Engineering at Sri Venkateswara University, Tirupati, Andhra Pradesh, India. He has completed B. Tech in Electronics and Communication Engineering from JNT University, Hyderabad, India and M.Tech in Communication and Signal Processing from Sri Krishnadevaraya University, Anantapur, India. He has Teaching & Industrial Experience of 6 years. His areas of Interest are Image and Signal Processing. He is a lifetime member of ISTE.